JACC Vol. 29, No. 1
January 1997:62–8

Assessment of Myocardial Viability in Chronic Coronary Artery Disease Using Technetium-99m Sestamibi SPECT

Correlation With Histologic and Positron Emission Tomographic Studies and Functional Follow-Up

ALEX F. MAES, MD, PHD, MARCEL BORGERS, PHD,*† WILLEM FLAMENG, MD, PHD, JOHAN L. NUYTS, PHD, FRANS VAN DE WERF, MD, PHD, FACC, JANNIE J. AUSMA, MSC,* PAUL SERGEANT, MD, PHD, LUC A. MORTELMANS, MD, PHD

Leuven and Beerse, Belgium and Maastricht, The Netherlands

Objectives. **The value of ^{99m}Tc-sestamibi (2-methoxy-isobutyl isonitrile [MIBI]) as a viability tracer was investigated in patients undergoing coronary artery bypass graft surgery.**

Background. **Initial studies claim that rest MIBI single-photon emission computed tomographic (SPECT) studies can be used to assess myocardial viability.**

Methods. **Thirty patients with a severely stenosed left anterior descending coronary artery and wall motion abnormalities were prospectively included. The patients underwent a MIBI rest study, a positron emission tomographic (PET) flow ($^{13}NH_3$) and metabolism (^{18}F-deoxyglucose) study and nuclear angiography before undergoing bypass surgery. A preoperative transmural biopsy specimen was taken from the left ventricular anterior wall. Morphometry was performed to assess percent fibrosis. After 3 months, radionuclide angiography was repeated.**

Results. **Statistically significant higher MIBI values were found in the group with myocardial viability as assessed by PET than in the group with PET-assessed nonviability ($p < 0.01$). Significantly higher MIBI values were found in the group with enhanced contractility at 3 months (76 ± 13% vs. 53 ± 22%, $p < 0.01$). A linear relation was found between MIBI uptake and percent fibrosis in the biopsy specimen ($r = 0.78$, $p < 0.00001$). When maximizing the threshold for assessment of viability with MIBI by using functional improvement as the reference standard, a cutoff value of 50% was found, with positive and negative predictive values of 82% and 78%, respectively.**

Conclusions. **^{99m}Tc MIBI uptake was significantly higher in PET-assessed viable areas and in regions with enhanced contractility at 3 months. A linear relation was found between percent fibrosis and MIBI uptake. An optimal threshold of 50% was found for prediction of functional recovery.**

(J Am Coll Cardiol 1997;29:62–8)

Positron emission tomography (PET) is known to accurately identify viable tissue in chronically ischemic myocardium (1–5). The principal limitations of PET imaging are the high costs of the equipment and the on site production of radiochemicals. Viability of myocardium can also be studied with high accuracy by using ^{201}Tl imaging reinjection or redistribution protocols (6–9). The possible role of ^{99m}Tc-sestamibi (2-methoxy-isobutyl isonitrile [MIBI]) is not clearly demonstrated in this context. Initial studies (10,11) claimed that rest MIBI single-photon emission computed tomographic (SPECT) studies could be used to obtain information on myocardial viability. More recently (12), quantified MIBI activity 1 h after injection was stated to be similar to redistribution ^{201}Tl activity, thus suggesting that MIBI is more than a pure flow tracer. The aim of this study was to assess the value of ^{99m}Tc MIBI as a viability tracer in patients with known coronary artery disease undergoing coronary artery bypass surgery and to correlate the findings in quantitative MIBI SPECT images with those of PET images and with quantitative histologic findings in biopsy specimens. For this purpose, patients with chronic coronary artery disease (CAD) and regional myocardial dysfunction undergoing bypass surgery were studied. Patients with left anterior descending coronary artery (LAD) disease were chosen so that a transmural biopsy specimen from the anterior free wall could be obtained easily without additional manipulation of the patient's heart.

From the Departments of Nuclear Medicine, Cardiovascular Surgery and Cardiology, K. U. Leuven, Leuven, Belgium; *Department of Molecular Cell Biology and Genetics, Cardiovascular Research Institute Maastricht, University of Limburg, Maastricht, The Netherlands; and †Janssen Research Foundation, Beerse, Belgium. This study was presented in part at the 45th Annual Scientific Session of the American College of Cardiology, Orlando, Florida, March 1996. It was supported by the Nationaal Fonds voor Wetenschappelijk Onderzoek, Brussels, Belgium and by the Advanced Clinical Research Award of the ADAC, Milpitas, California.

Manuscript received June 28, 1996; revised manuscript received August 28, 1996, accepted September 23, 1996.

Address for correspondence: Dr. Luc A. Mortelmans, Nuclear Medicine, UZ Gasthuisberg, Herestraat 49, 3000 Leuven, Belgium. E-mail (A Maes): Alex.Maes@uz.kuleuven.ac.be.

0735-1097/97/$17.00
PII S0735-1097(96)00442-1

Abbreviations and Acronyms

CAD = coronary artery disease
ECG = electrocardiogram
EF = ejection fraction
FDG = ^{18}F deoxyglucose
LAD = left anterior descending coronary artery
MIBI = sestamibi (2-methoxy-isobutyl isonitrile)
PET = positron emission tomography
ROI = region of interest
SPECT = single-photon emission computed tomography

Methods

Patient selection. Patients with known CAD, one- or two-vessel disease, an occlusion or severe stenosis (≥70%) of the LAD and anterior wall motion abnormalities were included prospectively. Patients with diabetes mellitus were excluded. The study protocol was granted approval by the ethical committee of the hospital (UZ Gasthuisberg, Leuven, Belgium). The same protocol for patient selection was used for other purposes in previous studies performed by our laboratory (13,14). No patient in this study has been previously reported on.

Coronary angiography and contrast ventriculography. All patients underwent contrast ventriculography and coronary angiography with the Sones technique within 8 weeks before operation. The ventriculograms and angiograms were visually interpreted by two experienced readers using the following scoring system: 1 = normokinesia; 2 = hypokinesia; 3 = severe hypokinesia, 4 = akinesia or dyskinesia. Interobserver variability was low, as the reviewers' scores differed for only two patients. A third reader scored the left ventriculograms in these patients and consensus was reached with the two other readers. Patients with severe stenosis of the LAD (≥70%) and hypokinesia, akinesia or dyskinesia on X-ray left ventricular angiography underwent radionuclide angiography.

Radionuclide angiography. One day before and 3 months after operation, nuclear angiography was performed for evaluation and follow-up of global and regional left ventricular function. Ten minutes after injection of 20 mCi of ^{99m}Tc-labeled red blood cells, equilibrium gated nuclear angiography was performed during 10 min while the patient was positioned under the gamma camera in a 45° left anterior oblique position. A low energy, all purpose collimator was used. The same study was repeated in a 70° left anterior oblique and an anterior position. Global and regional ejection fractions (EFs) were calculated by using standard software (Sopha Medical Benelux, Brussels, Belgium). End-diastolic and end-systolic regions of interest (ROIs) were determined automatically by convolving the end-diastolic image and a cycle summation image with an edge-enhancing kernel in the horizontal, vertical and two diagonal directions. Two binary images are produced that contain the positions of local maximums after each pass, yielding a closed border image after four passes. In these images, the left ventricular border is tracked to separate it from other outlined structures. The tracking starting point is the first border point to the right of the center of mass in a calculated contraction amplitude image. The final left ventricular ROI is the intersection of ROIs in both images (15,16). To calculate global EF, a background region is determined automatically as a ROI next to the free ventricular wall, following the outline of the left ventricular ROI. Background correction is done by simple subtraction. Global EF is calculated as End-diastolic volume − End-systolic volume/End-diastolic volume. To calculate regional EF, background correction is done by quadratic interpolation to compensate for nonhomogeneous tissue cross talk from the right ventricle, outflow tract and atrial appendages. Because no anatomic landmarks are visible in scintigraphic studies, the end-diastolic ROI is divided into eight "pie-shaped" sectors by using the center of mass of the end-diastolic left ventricular ROI as a center. The center remains the same during the whole cardiac cycle. The regions use overlapping image information (a region also uses half of the two adjacent regions). Regional EF is calculated by using the regional analog of End-diastolic volume − End-systolic volume/End-diastolic volume (15). The software was validated with 88 gated blood pool data sets from the Mayo Clinic against results obtained from the Mayo Clinic by their experienced technologists with their own software ($y = 0.87x + 6.2$, $r = 0.92$, x = Mayo Clinic software, y = Sopha program, SEE = 5.5, n = 88). Normal values for regional anterior EF with our software are 72 ± 5%. Regional function was considered to have improved if regional EF in the anterior wall was 5% higher at 3 months.

PET studies. In each patient, myocardial blood flow and metabolism were measured with PET 1 or 2 days before revascularization. The perfusion/metabolism studies were performed with a whole body positron emission tomograph (model 931-08/12, CTI Siemens). Before each study, a 2-min rectilinear scan, used to position the heart within the field of view, was followed by a 15-min transaxial transmission scan by using a ^{68}Ge ring source for photon attenuation correction.

Myocardial perfusion was evaluated by using^{13} NH_3 ammonia; 20 mCi of $^{13}NH_3$ in 5 ml of saline solution followed by a 20 ml flush of saline solution was slowly infused at a constant rate of 10 ml/min. Acquisition was started simultaneously with the injection of $^{13}NH_3$. In each patient, 19 dynamic frames were recorded (12 frames × 10 s, 4 × 30 s, 3 × 2 min). Total acquisition time was 10 min.

Regional myocardial utilization of exogenous glucose was evaluated with ^{18}F deoxyglucose (FDG). The metabolic studies were performed by using the euglycemic hyperinsulinemic clamp technique (17,18). Ten millicuries was injected 50 min after $^{13}NH_3$ injection. In each patient, 22 dynamic frames were recorded (8 frames × 15 s, 4 × 30 s, 2 × 1 min, 2 × 2 min, 6 × 10 min). Acquisition time was 70 min.

The 19 frames of the perfusion studies and the 22 frames of the metabolic studies were reconstructed, PET data were delineated and represented by using polar maps, using the central values between endocardial and epicardial contours, to minimize spillover from surrounding regions. (Using the max-

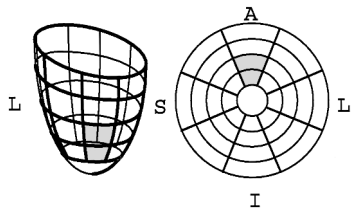

Figure 1. Example of a positron emission tomographic (PET) and ^{99m}Tc sestamibi (MIBI) polar map. There is a known 1:1 correspondence between sectors in the polar map and sectors in the delineated left ventricular wall. The **shaded sectors** are defined as the biopsy area; the mean value of this region was used for further analysis. A = anterior; I = inferior; L = lateral; S = septal.

imal value would result in increased spillover from the blood pool in the earlier frames [19].) Each polar map was divided into 33 sectors: 4 rings of 8 sectors and 1 sector for the apex. The average of the two sectors covering the region from which the biopsy specimen was taken (anterior wall) was used for further analysis (two shaded sectors in Fig. 1). To calculate absolute flow values from the tracer uptake curves of this region, a three-compartment model was applied (20,21). After absolute flow values were obtained with this model, a flow index was calculated as the ratio of the flow in the biopsy region divided by flow in the reference sector (no stenosis or stenosis <50% in the left circumflex or right coronary artery). Segments with flow values >80% of the flow value in the reference sector (flow index >0.8) were considered normal.

Regional glucose utilization values were estimated by applying a Patlak graphic analysis (22,23). The sector in which flow was considered to be normal was used as reference for FDG. A metabolic index, that is, the ratio of the glucose utilization in the biopsy region over that in the reference sector, was calculated.

Regions were defined as PET viable when the flow index was >0.8 or when the ratio of metabolic and flow index was >1.2. Regions were defined as PET nonviable when the flow index was <0.8 and when the ratio of metabolic and flow index was lower than 1.2. This criterion was previously established in normal volunteers (13,24,25).

Rest ^{99m}Tc MIBI SPECT studies. Patients underwent rest ^{99m}Tc MIBI SPECT studies 1 or 2 days before and 3 months after operation. ^{99m}Tc MIBI, 15 mCi, was injected at rest 60 min before the start of acquisition and flushed with 10 ml of saline solution. Approximately 10 min after injection, patients drank 20 cl of whole milk to enhance hepatic clearance of the isotope. The studies were performed on a three-head system (Trionix Triad XLT). Images were acquired with a ultrahigh resolution parallel hole collimator. The camera was rotated over a 120° orbit; and 24 projection images per head (1 min/projection) were obtained, resulting in 72 projections over 360°. A 20% window centered on the 140-ke V peak was used. The raw MIBI projections were processed with a two-dimensional Butterworth filter with a 0.52 cutoff and an order of 5, and reconstructed with a ramp filter. No attenuation correction was performed.

The MIBI images were delineated with the same procedure applied to the PET images, and polar maps were constructed by using the maximal pixel value between the endocardial and epicardial contours (19). For quantification of the results, the counts in the polar maps were normalized to the maximal value of the entire map. Because the polar maps have the same size and orientation as the PET flow and metabolic maps, the same region used in the PET studies (two shaded sectors in Fig. 1) was applied to the MIBI map, and the mean value of that region was used for further analysis of ^{99m}Tc MIBI uptake.

Microscopic examination. During operation, one transmural biopsy specimen was taken from the anterior wall of the left ventricle, approximately 4 cm from the apex, between the distal LAD and the last diagonal branch (Tru-Cut biopsy needle, Travenol Laboratories). The specimen was fixed in glutaraldehyde, postfixed in an OsO_4 solution and routinely embedded in epoxy resin. From each endocardial and epicardial part, semithick sections (2 μm) were examined with light microscopy. These results were pooled, because resolution of both PET and MIBI images preclude differentiation between the endocardial and epicardial parts of the myocardium. To assess the amount of connective tissue in the myocardium, a grid consisting of vertical and horizontal lines providing 121 intersections (points) was used. This morphometric technique has been used in previous studies (13,26,27). Counting the number of points overlying a certain structure results in quantitative determination of the volume of the structure under investigation in relation to the volume of the entire tissue under the square grid. The total number of points was regarded as 100%, and the points counted in the connective tissue were expressed as the percent of the entire tissue within the limits of the grid. The axis of the grid was then rotated ~45° and the same procedure was repeated. The analysis was reperformed on a different area of the same section. Longitudinal sections at magnification ×250 were evaluated.

Statistical analysis. Results are given as mean value ± SD. Differences between groups were investigated by using Student *t* tests for paired data. For evaluation of the relation between Tc99m sestamibi uptake or normalized PET flow and percent fibrosis, linear regression plots were used. Differences between correlation coefficients were tested by using Fisher z transformations. Positive predictive values, negative predictive values, sensitivity and specificity were calculated. To calculate an optimal threshold for MIBI (100 − %false positive − %false negative) was maximized.

Results

Study patients. Thirty patients (25 men and 5 women with a mean age ± SD of 63 ± 14 years) with severe stenosis of the LAD (≥70%) were prospectively included (Table 1). Coronary artery bypass surgery was scheduled for 22 of the 30 patients because of stable angina, for 5 because of unstable angina and for 3 because of heart failure. Four patients had had a previous anterior infarction. Preoperatively, the contrast ventriculogram revealed regional hypokinesia in 8, severe hypokinesia in

Table 1. PET Flow and Glucose Uptake, Percent MIBI Uptake, Ventricular Function and Percent Fibrosis in Anterior Wall Biopsy Specimen

Pt. No.	LAD Stenosis (%)	Absolute PET Flow (ml/min per 100 g)	Absolute PET Glucose Uptake (μmol/min per 100 g)	MIBI (% max)	Regional EF (%)		Global EF (%)		Fibrosis (%)
					Preop	3 mo	Preop	3 mo	
1	80	55	33	49	43	41	36	36	19
2	90	65	39	54	22	26	32	37	49
3	90	52	71		49	66	42	50	30
4	90	44	30	25	31	26	38	34	43
5	80	23	13	19	17		37		79
6	90	38	21		44	27	43	26	73
7	70	58	33	80	43	52	65	73	35
8	TO	65	56		39	45	46	48	40
9	70	72	47	81	49	44	68	72	26
10	70	77	36		53		51		28
11	TO	57	52	49	25	62	36	40	17
12	80	67	28	84	67	75	72	79	23
13	80	60	43	70	31	35	42	39	36
14	90	38	16	25	28	17	31	23	88
15	90	19	9	36	24		36		65
16	90	66	51	88	63	70	52	54	10
17	STO	59	61		41	52	63	67	16
18	STO	39	12	36	25	21	35	29	58
19	90	32	21	38	17	15	31	27	49
20	80	85	49	72	47	55	52	55	27
21	70			86	46	59	55	61	9
22	70			66	38	46	41	47	39
23	80	83	56	76	47	42	51	48	25
24	STO	54	42	89	35	49	31	40	18
25	90			81	29	35	40	43	49
26	90	64	37	50	43	37	44	41	38
27	80			84	44	65	64	73	23
28	80	97	96	80	61	53	64	66	11
29	90	60	46	66	45	40	50	46	29
30	80	90	54	85	44	51	47	53	10

EF = ejection fraction; LAD = left anterior descending coronary artery; MIBI (% max) = ^{99m}Tc sestamibi percent of peak activity; PET = positron emission tomography; PET flow = absolute regional myocardial blood flow; PET glucose = absolute myocardial glucose uptake; Preop = before coronary artery bypass surgery; Pt. = patient; STO = subtotal occlusion; TO = total occlusion; 3 mo = 3 months after coronary artery bypass surgery.

12 and akinesia or dyskinesia in 10 patients. Global and regional EF was followed up postoperatively with radionuclide angiography in 27 patients; in 13 global EF was improved and in 16, regional contractile function was improved. An electrocardiogram (ECG) was performed preoperatively and immediately after bypass surgery in all patients. If an ECG change was observed, cardiac enzymes were measured. With use of this routine procedure, no perioperative myocardial infarction was discovered in the study patients. In 5 of the 30 patients no MIBI imaging was performed and in 4 no PET images were acquired, owing to time constraints before scheduled cardiac surgery. Three patients refused follow-up measurements of left ventricular function.

Agreement between MIBI and different viability tracers. We first examined the general agreement between ^{99m}Tc MIBI findings and the results of PET, histologic studies and functional recovery studies.

^{99m}Tc MIBI percent of peak values was compared for PET-viable and PET-nonviable groups. Statistically significant higher MIBI values were found in the PET-viable than in the PET nonviable group (77 ± 15% [n = 6] vs. 53 ± 22% [n = 15], p = 0.02). A linear relation was found between MIBI uptake and PET-normalized $^{13}NH_3$ uptake values (y = 0.92x + 0.05, y = MIBI uptake, x = PET-normalized $^{13}NH_3$ uptake, n = 21, r = 0.83, p < 0.0001).

The percent fibrosis versus ^{99m}Tc MIBI percent of peak activity is represented in Figure 2. A significant inverse linear relation was found between MIBI uptake and the amount of fibrotic tissue in the biopsy specimen (y = −0.73x + 81; y = percent fibrosis, x = MIBI uptake, n = 25, r = 0.78, p < 0.00001). A similar relation was also observed between normalized PET perfusion data and percent fibrosis (y = −0.88x + 89, y = percent fibrosis, x = PET flow index, n = 26, r = 0.79, p < 0.00001) (Fig. 2). No significant difference was found between the correlation coefficients of both curves (p = NS).

Figure 3 shows ^{99m}Tc MIBI percent of peak activity for the patients with functional recovery and for those who had no improvement in regional left ventricular function. Significantly higher MIBI values were found in the group with enhanced

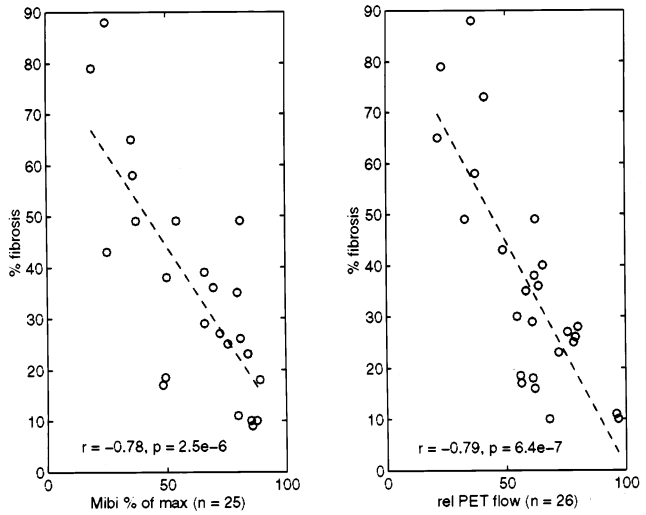

Figure 2. Percent fibrosis in anterior wall biopsy specimen versus ^{99m}Tc sestamibi (Mibi) **(left)** and versus normalized $^{13}NH_3$ uptake (rel PET flow) **(right)**. Mibi % of max = ^{99m}Tc sestamibi percent of peak activity. **Open circles** indicate individual data points.

regional EF at 3 months (^{99m}Tc MIBI uptake 76 ± 13% [n = 13] vs. 53 ± 22% [n = 10], $p < 0.01$). Similar results were obtained when analyzing MIBI uptake in relation to global EF (^{99m}Tc MIBI uptake 76 ± 14% [n = 11] vs. 56 ± 22% [n = 12], $p < 0.05$).

In Table 1, PET absolute regional myocardial blood flow and glucose uptake, percent MIBI uptake, percent fibrosis and functional evolution (regional EF and global EF) are plotted for each patient.

Predictive value of MIBI as viability tracer (Table 2). Because, by inclusion criteria, the left ventricular anterior wall was hypoakinetic or akinetic in each patient and because the biopsy specimen was taken from the anterior wall (4 cm from the apex) and MIBI values in the anterior wall were used for analysis, we used the evolution of regional EF as the reference standard to calculate an optimal threshold for MIBI. This threshold was calculated by maximizing (100 − % false positives − % false negatives). With this criterion, an optimal threshold of 50% was found. Significantly less fibrosis was found in the group with >50% MIBI uptake than in those with ≤50% MIBI uptake ($p < 0.01$, Fig. 4). When the 50% threshold was applied to the study, the positive predictive value was 82% and the negative predictive value was 78% (n = 23). In a study employing ^{201}Tl (28), a 50% cutoff was also found to be a valid value for viability assessment when quantitating ^{201}Tl uptake for prediction of improved function.

In contrast, positive and negative predictive values of 91%

Table 2. Comparison of MIBI and PET Findings With Functional Follow-Up Data

	Functional Improvement*	
	Yes (no. of pts.)	No (no. of pts.)
MIBI		
>50%†	12	4
≤50%	1	6
$^{13}NH_3$		
>50%†	11	5
≤50%	1	6
PET		
Viable anterior wall areas	10	1
Nonviable anterior wall areas	2	10

*Defined as improvement in regional ejection fraction. †50% was the optimal threshold for this study by maximizing (100 − %false positives − %false negatives). MIBI = ^{99m}Tc sestamibi percent of peak activity >50% or ≤50%; $^{13}NH_3$ = normalized positron emission tomography (PET) flow >50% or ≤50%; pts. = patients; other abbreviations as in Table 1.

Figure 3. ^{99m}Tc sestamibi (Mibi) uptake correlated with observed improvement or no improvement of regional ejection fraction. % of max = percent of peak activity. **Open circles** indicate individual data points.

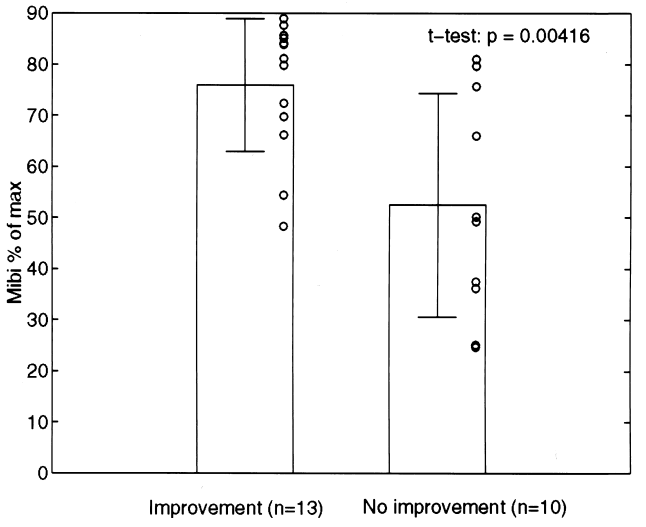

Figure 4. Percent fibrosis in anterior wall biopsy specimen in regions with ^{99m}Tc sestamibi (Mibi) uptake >50% and ≤50% of peak activity. **Open circles** indicate individual data points.

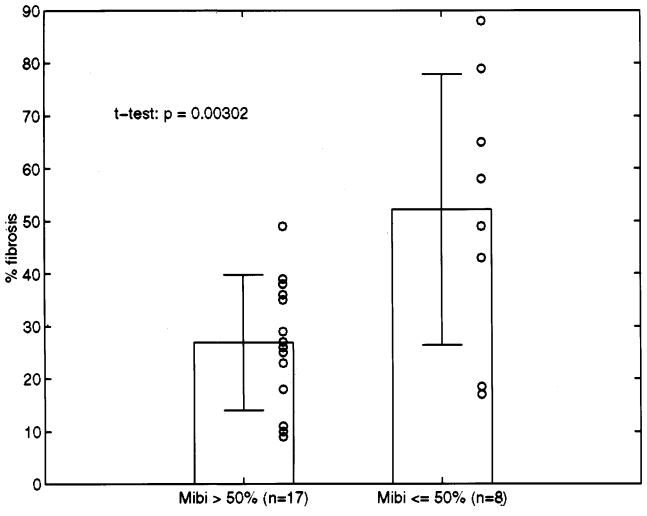

and 83%, respectively, were found for the PET match/mismatch model, with a sensitivity of 83% and a specificity of 91%. Additionally, predictive values for $^{13}NH_3$ flow for prediction of improved function were separated out from the overall PET criteria of flow and glucose uptake for viability. With use of the same formula as described earlier (maximizing 100 − %false positives − %false negatives), a threshold of 50% was found, resulting in positive and negative predictive values of 69% and 86% respectively, with a sensitivity of 92% and a specificity of 55%.

Discussion

In this study, we examined whether ^{99m}Tc MIBI can play a role in the assessment of myocardial viability. Statistically significant higher MIBI uptake values were found in areas with PET-assessed myocardial viability and in regions that revealed improvement of left ventricular function 3 months after coronary artery bypass surgery, suggesting a possible role for MIBI as viability tracer. Moreover, a linear relation was found between percent fibrosis and MIBI uptake ($r = 0.78$). In a recent study (29), a similar linear relation was found between percent fibrosis and thallium activity after tracer reinjection ($r = 0.85$), whereas the correlation between thallium activity and fibrosis was lower when only conventional redistribution images were considered ($r = 0.62$). These data suggest that quantitative analysis of regional activity of ^{99m}Tc MIBI after rest injection provides information on the amount of interstitial fibrosis comparable to that of regional activity of ^{201}Tl after reinjection. A significant relation between the amount of connective tissue in the biopsy specimen and PET-normalized flow values was found ($r = 0.79$), suggesting that perfusion levels alone, as traced by $^{13}NH_3$, are also an indicator of the amount of fibrotic tissue. This finding is in concordance with the hypothesis (30) that hibernating myocardium is the result of repetitive episodes of ischemia with a persistent stunning effect and normal or near normal blood flow values in the hypocontractile area. It has also been shown (31) that retention of $^{13}NH_3$ requires the presence of viable myocardial cells.

When we considered recovery of regional left ventricular function as a reference standard for viability, we found an optimal threshold of 50% for MIBI, resulting in positive and negative predictive values of 82% and 78%, respectively. This finding is in concordance with previous studies (32–34) indicating that MIBI kinetics appear to depend on cell membrane integrity and mitochondrial respiration. When a threshold is used to assess myocardial "viability," it is necessary to recognize that myocardial viability is a continuum (35). Myocardial segments with decreased tracer uptake may contain a substantial amount of viable myocardium. The 50% threshold used relates to the likelihood of improvement of regional wall motion after revascularization.

Concerning the comparison between PET flow imaging and ^{99m}Tc MIBI for the detection of viability, relatively low specificity values were found for both when using a cutoff value of 50%. This finding is in agreement with recent work (36) indicating that functional recovery can be predicted when using $^{13}NH_3$ at low uptake (<40%) and high uptake (>80%) values, whereas intermediate normalized flow values necessitate additional information regarding glucose or oxidative metabolism to estimate accurately the potential for recovery.

Positive and negative predictive values for PET NH_3/FDG imaging in this study were higher (83% and 91%, respectively) than the values for $^{13}NH_3$ alone and the values for ^{99m}Tc MIBI, indicating an added value for the NH_3/FDG match/mismatch model for the detection of viable segments. However, one should also consider the limited availability of PET centers or cyclotron sites and the relatively high cost of the investigation.

The most important limitation of this study is that it is not absolutely certain that myocardial anterior wall segments defined by the MIBI SPECT studies correspond exactly to the PET segments and that histologic results derived from a small biopsy specimen (~15 mg) can be extrapolated to data on metabolism, flow and function for much larger areas. However, the three-dimensional delineation of both MIBI and PET images resulted in accurate mapping of the anatomic location of each region. It should also be noted that our data apply only to patients with CAD in whom viability of the anterior wall is being assessed.

From the preceding analysis, one may conclude that the level of ^{99m}Tc MIBI uptake is linearly related to the amount of interstitial fibrosis. When using left ventricular functional improvement as the standard for viability, we found an optimal threshold of 50% for MIBI with positive and negative predictive values of 82% and 78%, respectively. Therefore, the present data indicate that MIBI reflects not only flow, but also, at least in part, myocardial viability.

References

1. Schelbert HR, Buxton D. Insights into coronary artery disease gained from metabolic imaging. Circulation 1988;78:496–505.
2. Marwick HT, MacIntyre JW, Salcedo EE, Go RT, Saha G, Beachler A. Identification of ischemic and hibernating myocardium: feasibility of post-exercise F-18-deoxyglucose positron emission tomography. Cathet Cardiovasc Diagn 1991;22:100–6.
3. Tamaki N, Yonekura Y, Yamashita K, et al. Positron emission tomography using fluorine-18-deoxyglucose in evaluation of coronary artery bypass grafting. Am J Cardiol 1989;64:860–5.
4. Tillisch J, Brunken R, Marshall R, et al. Reversibility of cardiac wall motion abnormalities predicted by positron tomography. N Engl J Med 1986;314:884–8.
5. Nienaber CA, Brunken RC, Sherman CT, et al. Metabolic and functional recovery of ischemic human myocardium after coronary angioplasty. J Am Coll Cardiol 1991;18:966–78.
6. Dilsizian V, Perrone-Filardi P, Arrighi JA, et al. Concordance and discordance between stress-redistribution -reinjection and rest-redistribution thallium imaging for assessing viable myocardium. Comparison with metabolic activity by positron emission tomography. Circulation 1993;88:941–52.
7. Kayden DS, Sigal S, Soufer S, Mattera J, Zaret BL, Wackers FJ. Thallium-201 for assessment of myocardial viability: quantitative comparison of 24-hour redistribution imaging with imaging after reinjection at rest. J Am Coll Cardiol 1991;18:1480–6.
8. Soufer R, Dey HM, Lawson AJ, Wackers FJ, Zaret BL. Relationship between reverse redistribution on planar thallium scintigraphy and regional myocardial viability: a correlative PET study. J Nucl Med 1995;36:180–7.

9. Bonow RO, Dilsizian V, Cuocolo A, Bacharach SL. Identification of viable myocardium in patients with chronic coronary artery disease and left ventricular dysfunction. Comparison of thallium scintigraphy with reinjection and PET imaging with 18F-fluorodeoxyglucose. Circulation 1991;83:26–37.
10. Rocco TP, Dilsizian V, Strauss HW, Boucher CA. Technetium-99m isonitrile myocardial uptake at rest. II. Relation to clinical markers of potential viability. J Am Coll Cardiol 1989;14:1678–84.
11. Maurea S, Cuocolo A, Pace L, et al. Left ventricular dysfunction in coronary artery disease: comparison between rest-redistribution thallium 201 and resting technetium 99m methoxyisobutyl isonitrile cardiac imaging. J Nucl Cardiol 1994;1:65–71.
12. Udelson JE, Coleman PS, Metherall J, et al. Predicting recovery of severe regional ventricular dysfunction. Comparison of resting scintigraphy with 201Tl and 99mTc-sestamibi. Circulation 1994;89:2552–61.
13. Maes A, Flameng W, Nuyts J, et al. Histological alterations in chronically hypoperfused myocardium: correlation with PET findings. Circulation 1994; 90:735–45.
14. Shivalkar B, Maes A, Borgers M, et al. Only hibernating myocardium invariably shows early recovery after coronary revascularization. Circulation 1996;94:308–15.
15. Goris ML, Briandet PA. A Clinical and Mathematical Introduction to Computer Processing of Scintigraphic Images. New York: Raven Press, 1983:143–4, 172–6, 182–9.
16. Goris ML, McKillop JH, Briandet PA. A fully automated determination of the left ventricular region of interest in nuclear angiocardiography. Cardiovasc Intervent Radiol 1981;4:117–23.
17. Knuuti JM, Nuutila P, Ruotsalainen U, et al. Euglycemic hyperinsulinemic clamp and oral glucose load in stimulating myocardial glucose utilization during positron emission tomography. J Nucl Med 1992;33:1255–62.
18. DeFranzo RA, Tobin JD, Andres R. Glucose clamp technique: a method for quantifying insulin secretion and resistance. Am J Physiol 1979;237:E214–23.
19. Nuyts J, Suetens P, Oosterlinck A, De Roo M, Mortelmans L. Delineation of ECT images using global constraints and dynamic programming. IEEE Trans Med Imaging 1991;10:489–98.
20. Muzik O, Beanlands RS, Hutchins GD, Mangner TJ, Nguyen N, Schwaiger M. Validation of nitrogen-13-ammonia tracer kinetic model for quantification of myocardial blood flow using PET. J Nucl Med 1993;34:83–91.
21. Nuyts J, Maes A, Vrolix M, et al. Three-dimensional correction for spill-over and recovery of myocardial PET images. J Nucl Med 1996;37:767–74.
22. Patlak CS, Blasberg RG, Fenstermacher JD. Graphical evaluation of blood-to-brain transfer constants from multiple-time uptake data. J Cereb Blood Flow Metab 1983;3:1–7.
23. Patlak CS, Blasberg RG. Graphical evaluation of blood-to-brain transfer constants from multiple-time uptake data generalizations. J Cereb Blood Flow Metab 1985;5:584–90.
24. De Landsheere C, Raets D, Pierard L, et al. Regional myocardial perfusion and glucose uptake: clinical experience in 92 cases studied with positron tomography. In: Schmidt HAE, Chambron J, editors. Nuclear Medicine: Quantitative Analysis in Imaging and Function. Stuttgart: Schattaue Verlag, 1990:245–7.
25. Maes A, Van de Werf F, Nuyts J, Bormans G, Desmet W, Mortelmans L. Impaired myocardial tissue perfusion early after successful thrombolysis. Impact on myocardial flow, metabolism and function at late follow-up. Circulation 1995;92;2072–8.
26. Schwartz F, Flameng W, Theidemann KU, Schaper W, Schlepper M. Effect of coronary stenosis on myocardial function, ultrastructure and aortocoronary bypass grafting hemodynamics. Am J Cardiol 1987;42:193–201.
27. Borgers M, Thone F, Wouters L. Ausma J, Shivalkar B, Flameng W. Structural correlates of regional myocardial dysfunction in patients with critical artery stenosis: chronic hibernation? Cardiovasc Pathol 1994;2:237–45.
28. Ragosta M, Beller GA, Watson DD, Kaul S, Gimple LW. Quantitative planar rest-redistribution 201Tl imaging in detection of myocardial viability and prediction of improvement of left ventricular function after coronary bypass surgery in patients with severely depressed left ventricular function. Circulation 1993;87:1630–41.
29. Zimmermann R, Mall G, Rauch B, et al. Residual 201TL activity in irreversible defects as a marker of myocardial viability. Circulation 1995;91: 1016–21.
30. Vanoverschelde JL, Wijns W, Depre C, et al. Mechanisms of chronic regional postischemic dysfunction in humans. New insights from the study of noninfarcted collateral-dependent myocardium. Circulation 1993;87,1513–23.
31. Rauch BR, Helus F, Grunze M, Braunwell E, Hasselbach W, Kubler W. Kinetics of 13N-ammonia in myocardial single cells indicating potential limitations in its applicability as a marker of myocardial blood flow. Circulation 1985;71:387–93.
32. Piwnica-Worms D, Kronauge JF, Chiu ML. Uptake and retention of hexakis (2-methoxyisobutyl isonitrile) technetium(I) in cultured chick myocardial cells. Mitochondrial and plasma membrane potential dependence. Circulation 1990;82:1826–38.
33. Piwnica-Worms D, Chiu ML, Kronauge JF. Divergent kinetics of 201Tl and 99mTc-sestamibi in cultured chick ventricular myocytes during ATP depletion. Circulation 1992;85:1531–41.
34. Beanlands RS, Dawood F, Wen WH, et al. Are the kinetics of technetium-99m methoxybutyl isonitrile affected by cell metabolism and viability? Circulation 1990;82:1802–14.
35. Wackers FJ. Radionuclide detection of myocardial ischemia and viability: is the glass half empty or half full? J Am Coll Cardiol 1996;27:1598–600.
36. Duvernoy CS, vom Dahl J, Laubenbacher C, Schwaiger M. The role of nitrogen 13 ammonia positron emission tomography in predicting functional outcome after coronary revascularization. J Nucl Cardiol 1995;2:499–506.